Raman scattering from the spin-gap mode in the Ni-doped spin-Peierls compound $CuGeO_3$

Tomoyuki Sekine,* Tomomi Kaneko, and Haruhiko Kuroe
Department of Physics, Sophia University, 7-1 Kioi-cho, Chiyoda-ku, Tokyo 102-8554, Japan

Takatsugu Masuda
International Graduate Schools of Arts and Sciences, Yokohama City University, 22-2 Seto, Kanazawa-ku, Yokohama 236-0027, Japan
(Received 20 November 2007; revised manuscript received 3 June 2008; published 10 October 2008)

By means of Raman scattering we have studied the spin-Peierls (SP) transition in Ni-doped $CuGeO_3$ crystals. The folded-phonon peak extremely broadens and the two-magnetic-excitation mode disappears when the Ni concentration is above about 2.0%, indicating that the SP phase collapses. The spin-gap mode is activated in lightly Ni-doped samples. This peak neither splits nor shifts under magnetic fields in the SP phase, but its frequency increases in the incommensurate phase. The activation of the spin-gap mode is interpreted in terms of a mixing between the spin-singlet ground state and the $S_z=0$ triplet excited one by staggered fields around the doped impurities. Meanwhile, the two-magnetic-excitation mode gradually diminishes in intensity with increasing magnetic field in the incommensurate phase.

DOI: 10.1103/PhysRevB.78.134409 PACS number(s): 75.90.+w, 78.30.−j

I. INTRODUCTION

The report on the spin-Peierls (SP) transition at $T_{SP} \simeq 14$ K in an inorganic compound $CuGeO_3$ by Hase, Terasaki, and Uchinokura[1,2] has rekindled significant interest in the instability of quantum spin-1/2 antiferromagnetic (AF) chains to the spin-singlet ground state together with a lattice dimerization, i.e., the SP state. This compound consists of spin chains of Cu^{2+} ions running along the crystallographic c axis, where the spins of these Cu^{2+} ions are coupled by antiferromagnetic superexchange interactions via the oxygen orbitals. The spin system can be modeled by the one-dimensional Hamiltonian

$$\mathcal{H} = J\sum_i \{(1+\gamma)\boldsymbol{s}_{2i-1}\cdot\boldsymbol{s}_{2i} + (1-\gamma)\boldsymbol{s}_{2i}\cdot\boldsymbol{s}_{2i+1} + \alpha(\boldsymbol{s}_{2i-1}\cdot\boldsymbol{s}_{2i+1} + \boldsymbol{s}_{2i}\cdot\boldsymbol{s}_{2i+2})\}, \quad (1)$$

where γ (>0) is the temperature-dependent dimerization parameter that vanishes in the homogeneous state above T_{SP}. In $CuGeO_3$ a next-nearest-neighbor frustration term αJ is competing with the nearest-neighbor exchange interaction J.

The discovery of an inorganic SP compound $CuGeO_3$ gives an ability to easily introduce dopants, which allows us to study systematically the impurity effects on the SP transition. The first study on the effects of Zn substitution for Cu on the SP transition of $CuGeO_3$ was done by Hase *et al.*[3] After this study two kinds of doping have been carried out: one is to directly change the spin degrees of freedom within each CuO_2 chain by replacing some of the Cu^{2+} ions ($s=1/2$) with nonmagnetic impurities (Zn^{2+}, Mg^{2+}, etc.) or magnetic impurities (Ni^{2+} possessing $s=1$, etc.). The other is by substituting Si for Ge, which modifies the strength of the exchange interactions between the magnetic ions.

It has been established by many experimental works that the impurity doping suppresses the occurrence of the SP transition and activates an underlying AF phase transition.[3–8] When the dopant concentration is below a few percent, the formation of the AF long-range order on the spin-gap background was confirmed by neutron scattering.[9–12] The electron spin resonance (ESR) results[13,14] indicate that the SP and AF phases coexist just below the Néel temperature T_N, but there is no phase separation between them enough below T_N, i.e., the dimerized AF phase is formed at low temperatures. At high dopant concentrations, the long-range SP order disappears and the uniform AF phase without the lattice dimerization is stabilized. Masuda *et al.*[15] studied magnetic susceptibility in Mg-doped crystals and stated that a compositional first-order phase transition between the dimerized and uniform AF phases occurred at a critical concentration x_c and consequently the Néel temperature T_N exhibited a conspicuous jump.

Fukuyama *et al.*[16] studied theoretically the impurity-doped SP state, especially when the exchange interactions near impurities are modified in Si-doped $CuGeO_3$, using the phase Hamiltonian technique. They stated that the envelopes of the staggered AF moment and the lattice dimerization expressed by elliptic functions were formed in the dimerized AF state, which was ascertained by μSR experiment.[17]

The Ni^{2+} ion possesses a spin of $s=1$. Its dopant concentration-temperature phase diagram is qualitatively similar to that of the nonmagnetic-impurity-doped $CuGeO_3$, i.e., Zn-, Mg-, and Si-doped samples.[18–22] It was reported in the susceptibility study of $Cu_{1-x}Ni_xGeO_3$ that the long-range SP order disappeared above a critical concentration $x_c \cong 0.020$, and the uniform AF state without lattice dimerizations was formed at low temperatures.[18,19] However, the Néel temperature T_N rapidly decreased with decreasing Ni concentration just below x_c. Contrary to other impurities, the easy axis is directed nearly along the a axis in the AF state because of the single-ion anisotropy, which is a distinguishing feature in Ni-doped sample.[18,19,21–23] In this case it is important to study the nature of the ground state and excitations in order to understand the doped SP state.

The application of a magnetic field on the SP state of pure or impurity-doped samples reduces the spin-gap energy of the lowest triplet state in the magnetic excitation spectrum, and at the critical field H_c a transition to an incommensurate (IC) state takes place with an occurrence of finite magnetization.[24]

Raman scattering is one of the useful experimental methods to observe elementary excitations and study the SP transition.[25–27] In the SP phase of pure $CuGeO_3$, some characteristic Raman peaks, i.e., the folded-phonon modes[26] and the two-magnetic-excitation bound state, were observed.[27] The emergence of the former indicates the formation of the lattice dimerization. The latter is created just below double the SP-gap energy by a strong attractive interaction between two magnetic excitations. The SP-gap mode, i.e., the spin-gap mode, is not observed in the first-order Raman process in pure $CuGeO_3$. However, it becomes Raman active in lightly Zn-, Mg-, and Si-doped $CuGeO_3$.[27–31] Els *et al.*[28,32] interpreted this Raman peak in terms of the mobile dopant-bound spinons. Loa *et al.*[29,30] stated that it was attributed to the spin-gap mode which was activated by a spinon-assisted process.

The spin-gap mode in pure $CuGeO_3$ was also observed in the IC phase by means of Raman scattering under high magnetic fields.[29,30,33] Moreover, the two-magnetic-excitation bound state gradually disappeared as the magnetic field was increased in the IC phase.

It seems to us that the Raman process of emergence of the spin-gap mode from the doped SP state and the IC phase in pure $CuGeO_3$ has not been satisfactorily clarified yet. Raman scattering in Ni-doped SP system provides additional information on the nature of their ground states and magnetic and phononic excitations.

II. EXPERIMENT

Single crystals of Ni-doped samples, $Cu_{1-x}Ni_xGeO_3$, were grown by the floating-zone method. The impurity concentration x in the Ni-doped $CuGeO_3$ was determined and the homogeneity was checked by inductively coupled plasma atomic emission spectroscopy (ICP-AES). Raman spectra in the right-angle scattering geometry were excited using the Ar^+-ion laser lines. The $b(c,c)a$, $b(c,b+c)a$, and $a(c,a+c)b$ spectra, dispersed by a Jobin-Yvon U1000 double-grating monochromator, were detected by a photon counting system because the folded phonons and magnetic excitations appear in the (c,c) polarization configuration.[25,27] Here, the notation of the crystal axes follows the convention of Völlenkle *et al.*[34] The samples were cooled by a helium-gas-flow-type cryostat with temperature regulation better than ± 0.3 K. The magnetic field was applied along the a and b axes using a split-type superconducting magnet (Oxford Instruments, Spectromag) with temperature regulation better than ± 0.1 K.

III. RESULTS

In the SP state, an energy gap between the singlet ground and triplet excited states opens and a lattice dimerization is formed. By Raman scattering we observed specific excitations in the SP state of pure $CuGeO_3$, i.e., the folded-phonon modes and the two-magnetic-excitation bound state.[25–28] Moreover, the spin-gap mode was observed in lightly doped $CuGeO_3$.[27,28]

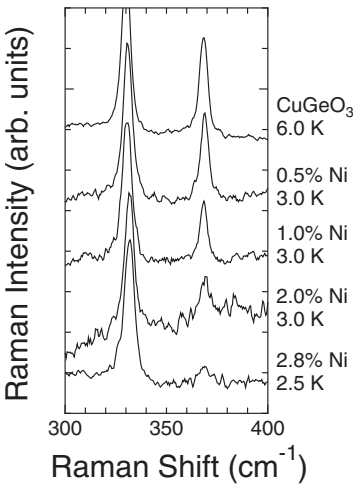

FIG. 1. The $b(c,c)a$ Raman spectra between 300 and 400 cm^{-1} in pure and Ni-doped $CuGeO_3$ crystals at low temperatures.

A. Folded phonons

First, let us show Raman spectra from the folded-phonon mode between 300 and 400 cm^{-1} in pure and Ni-doped $CuGeO_3$ in Fig. 1. Two peaks at 330 and 369 cm^{-1} are assigned to a Raman-active A_g-phonon mode and a folded-phonon mode, respectively. The folded-phonon mode is folded from the Brillouin-zone boundary onto the zone center in the SP state. Consequently it is indicative of the formation of the lattice dimerization by the SP transition. At the critical concentration $x_c \simeq 0.020$, we observed a weak peak possessing a broad structure at the high-frequency side. A similar feature was observed in heavily Zn- and Si-doped samples,[26] which is due to the short-range lattice dimerization. At $x=0.028$ only a very weak and broad peak was observed, indicating that the long-range SP order was almost completely destroyed.

Figure 2 shows the temperature dependence of Raman spectra between 300 and 400 cm^{-1}. The folded-phonon mode at 369 cm^{-1} disappeared at 12 K in 0.5% Ni-doped sample and at 11 K in 1.0% one. These temperatures are 1–1.5 degrees lower than the SP transition temperatures T_{SP}

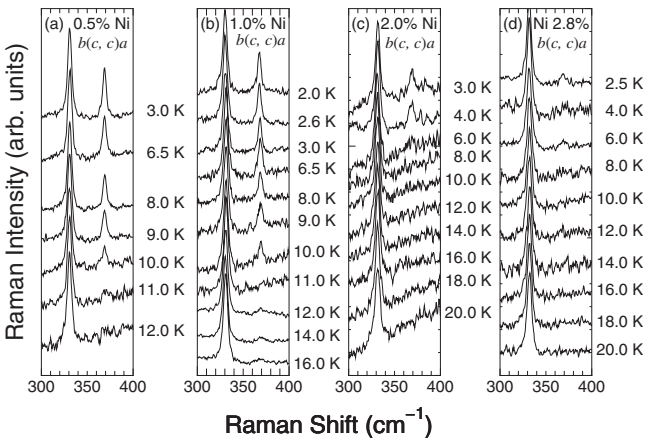

FIG. 2. Temperature dependence of Raman spectra between 300 and 400 cm^{-1} in Ni-doped $CuGeO_3$ crystals.

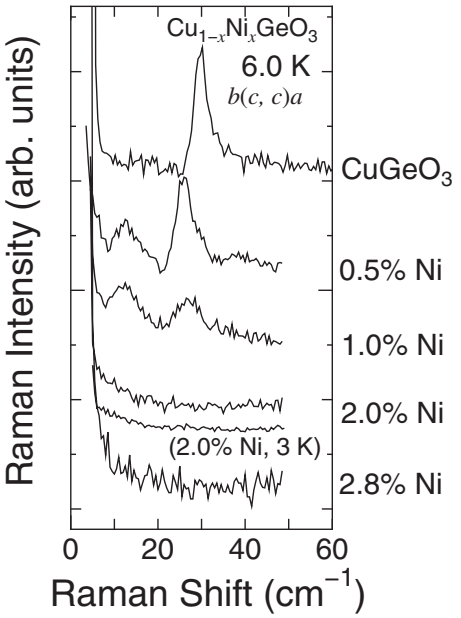

FIG. 3. Low-frequency Raman spectra at 6.0 K in pure and Ni-doped $CuGeO_3$ crystals. The spectrum at 3.0 K is also shown in 2.0% Ni-doped sample.

estimated by the magnetic susceptibility.[18,19] Only a broad structure was observed below 4 K in 2.0% and 2.8% Ni-doped samples, indicating that the long-range SP order was not formed even at low temperatures.

B. Magnetic excitations

Figure 3 shows the low-frequency Raman spectra at 6.0 K in pure and Ni-doped $CuGeO_3$ crystals. In pure sample an asymmetric sharp peak was observed at about 30 cm^{-1} and assigned as a two-magnetic excitation bound state. It is created just below double the SP-gap energy by a strong attractive interaction between two magnetic excitations. The intensity and peak position of the 30-cm^{-1} peak decrease, and the peak profile becomes symmetric as the Ni concentration is increased, which suggests a crossover from the two-magnetic-excitation bound state to the two-magnetic-excitation resonance one.[27] Hereafter, we call it the two-magnetic-excitation mode. In 0.5% and 1.0% Ni-doped samples, we observed the spin-gap mode at about 14 and 13 cm^{-1}, respectively, in the (c,c) polarization configuration together with the two-magnetic-excitation mode. It indicates that the SP-gap energy $\Delta(T)$ decreases with increasing Ni concentration, which is consistent with the result of neutron scattering.[35] The spin-gap mode becomes observable due to the Ni doping, as will be discussed later in detail. We emphasize that it has almost the same Raman intensity as the two-magnetic-excitation mode.

The observation of the two-magnetic-excitation mode and the spin-gap mode is a clear evidence of the opening of the SP gap in the magnetic excitation spectrum. However, they cannot be observed in 2.0% and 2.8% Ni-doped samples, indicating that the long-range SP order is not formed in these samples. It should be noted that the spin-gap mode was not observed at 3.0 K, while the broad folded-phonon mode appeared below 4.0 K in 2.0% Ni-doped sample, clearly indicating that the long-range SP order was not formed but the strong short-range lattice dimerization existed below 4.0 K.

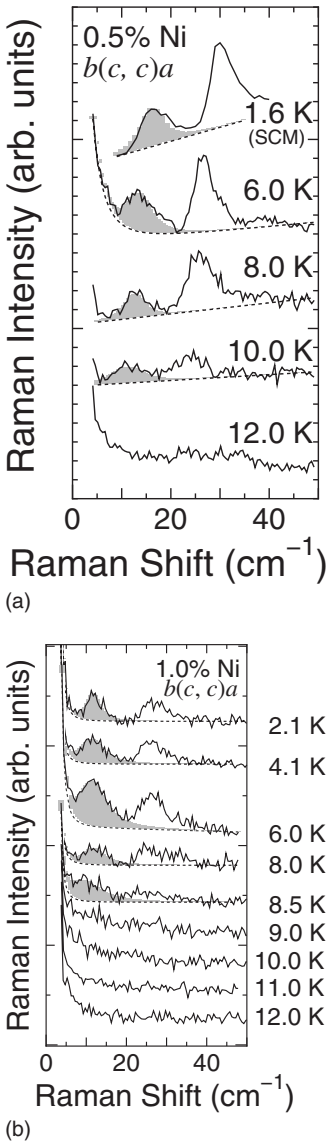

FIG. 4. Temperature dependence of the low-frequency Raman spectra in (a) 0.5 and (b) 1.0% Ni-doped $CuGeO_3$ crystals. The hatched areas denote the components of the spin-gap mode in the fitting, and the dotted curves denote the backgrounds and/or the direct scattering of incident light. Since the 1.6-K spectrum of 0.5% Ni-doped sample was obtained in the superconducting magnet (SCM), the intensity cannot be directly compared with the spectra at high temperatures. The optical alignment in the SCM was different from that in the helium-gas-flow-type cryostat.

Figure 4 shows temperature dependence of the low-frequency Raman spectra in 0.5 and 1.0% Ni-doped $CuGeO_3$ crystals. The spin-gap mode and the two-magnetic-excitation mode decrease in frequency with increasing temperature, and they disappear above T_{SP}. The frequency of the spin-gap mode and the peak position of the two-magnetic-excitation mode as functions of temperature are shown in Fig. 5. The former was obtained by fitting the spectrum in the method of

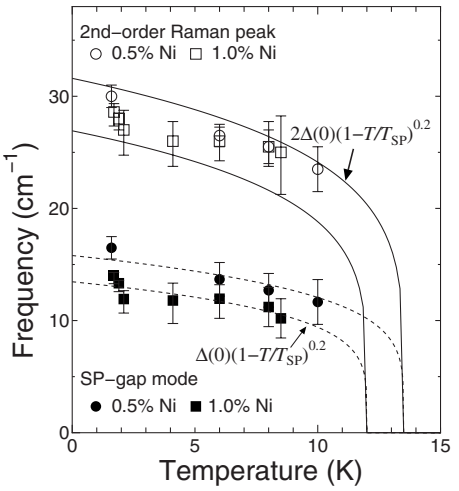

FIG. 5. Temperature dependence of the frequency of the spin-gap mode and the peak position of the two-magnetic-excitation mode in 0.5 and 1.0% Ni-doped $CuGeO_3$. The dashed curves denote power-law fits $\Delta(T)=\Delta(0)(1-T/T_{SP})^{\beta}$ using the results of magnetic susceptibility, $T_{SP}=13.5$ K and 12.0 K in 0.5 and 1.0% Ni-doped samples (Refs. 18 and 19). The solid curves denote $2\Delta(T)$.

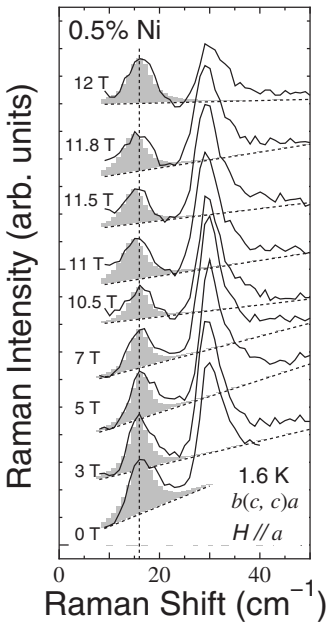

FIG. 6. Magnetic-field dependence of the low-frequency Raman spectrum at 1.6 K in 0.5% Ni-doped $CuGeO_3$, when the magnetic field is applied parallel to the a axis. The hatched areas denote the components of the spin-gap mode in the fitting, and the dotted lines denote the backgrounds. The vertical dotted line denotes the frequency of the spin-gap mode.

least-squares. Here we assumed that not only the spin-gap mode but also the two-magnetic-excitation mode and the tail of the direct scattering near zero cm^{-1} have Lorentzian curves. The obtained curve does not fit well the spectrum between the spin-gap and the two-magnetic-excitation modes, i.e., near 25 cm^{-1}, because the latter has an asymmetric line shape. The result omitting the component of the two-magnetic-excitation mode from the fitted curve is shown in Fig. 4, and the hatched area reproduces well the net component of the spin-gap mode. The SP-gap energy $\Delta(0)$ at $T=0$ K holds a relation of $\Delta(0)=Ck_BT_{SP}$ with $C=1.61$, which is slightly smaller than $C=1.76$ of BCS theory in superconductors.[27,31] The peak position of the two-magnetic-excitation mode is almost twice the frequency of the spin-gap mode in 0.5% Ni-doped sample, but the former seems to be a little bit larger than double the latter in 1.0% Ni-doped one. We think that it is explainable in terms of a crossover from the two-magnetic-excitation bound state to the two-magnetic-excitation resonance state, as well as Zn- and Si-doped samples.[27]

C. Magnetic-field effects

Figure 6 shows the magnetic-field dependence of the low-frequency Raman spectrum at 1.6 K in 0.5% Ni-doped $CuGeO_3$. The magnetic field is applied parallel to the a axis. The frequency of the spin-gap mode and the peak position of two-magnetic-excitation mode do not change when the magnetic field is applied, indicating that the IC phase transition does not occur below 12 T.

Figure 7(a) shows the magnetic-field dependence of the low-frequency Raman spectrum of 1.0% Ni-doped $CuGeO_3$ at 1.9 K in the $b(c,b+c)a$ configuration, when the magnetic field is applied parallel to the a axis. The detailed magnetic-field dependence of the $b(c,c)a$ Raman spectrum above 10 T at 1.7 K is shown in Fig. 7(b). The frequency of the spin-gap mode and the peak position of the two-magnetic-excitation mode increased above 11.5 T. Moreover, the two-magnetic-excitation mode decreased in intensity above 11.5 T.

The intensity of the spin-gap mode shows strange magnetic-field dependence. As seen in Fig. 7, it decreases at 5 T and becomes almost constant with increasing magnetic field. Then it increases above 11 T. It is noted that the change in the intensity is not due to the Faraday rotation of the scattered light, because the scattered light is collected without polarization analyzers in the $b(c,a+c)a$ polarization configuration in Fig. 7(a) and the wave vector of the incident light is perpendicular to the magnetic field. Moreover, each intensity of the spectrum in Fig. 7(a) was normalized by that of the 187-cm^{-1} A_g phonon peak.

Figure 8 shows the magnetic-field dependence of the low-frequency $a(c,a+c)b$ Raman spectrum of 1.0% Ni-doped $CuGeO_3$, when the magnetic field is applied parallel to the b axis. The spin-gap mode neither splits nor shifts in the SP phase when the magnetic fields are applied parallel to the a and b axes.

Figures 9(a) and 9(b) show the magnetic-field dependence of the frequency of the spin-gap mode and the peak position of the two-magnetic-excitation mode in 0.5% and 1.0% samples, respectively. The frequency of the spin-gap mode in 0.5% and 1.0% Ni-doped samples was determined by fitting the spectrum, as described above. One can see that the frequencies of the spin-gap mode and the two-magnetic-excitation mode increase above about 11.5 T in 1.0% Ni-doped $CuGeO_3$, which indicates that the IC phase transition occurs at $H_c \simeq 11.5$ T and the critical magnetic field H_c decreases with increasing Ni concentration.

With respect to the spin-gap mode and the two-magnetic-excitation mode, almost the same results as the present ones

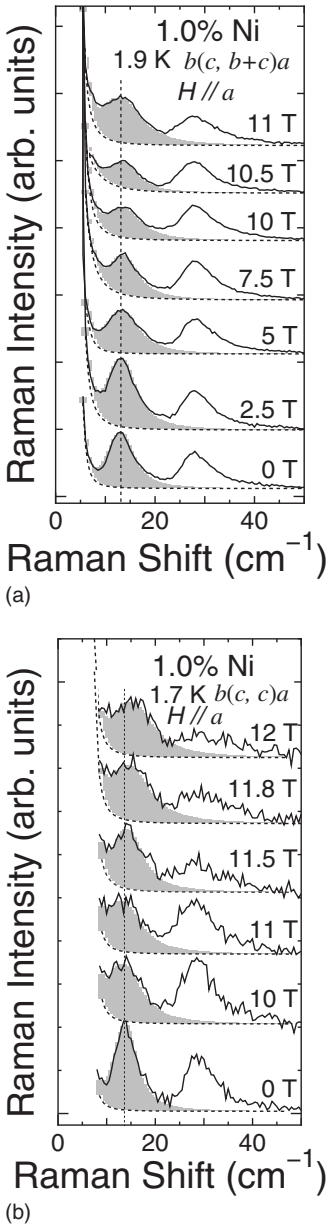

FIG. 7. (a) Magnetic-field dependence of the low-frequency $b(c,b+c)a$ Raman spectrum at 1.9 K and (b) the details of the $b(c,c)a$ Raman spectrum above 10 T at 1.7 K in 1.0% Ni-doped $CuGeO_3$, when the magnetic field is applied parallel to the a axis. The hatched areas denote the components of the spin-gap mode in the fitting, and the dotted curves denote sums of the direct scattering of incident light and the background. The dotted vertical lines denote the frequency of the spin-gap mode under low magnetic fields.

were observed in the Raman scattering of Si-doped $CuGeO_3$ under high magnetic fields by Loa.[30] He and his coworkers also studied Raman scattering of pure $CuGeO_3$ under high magnetic fields and reported that the spin-gap mode was activated in the IC phase, while it is Raman inactive in the SP phase.[29,30,33] Moreover, the two-magnetic-excitation bound state gradually disappeared as the magnetic field was increased in the IC phase.

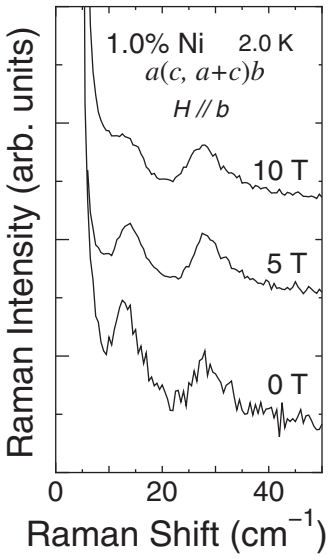

FIG. 8. Magnetic-field dependence of the low-frequency $a(c,a+c)b$ Raman spectrum at 2.0 K in 1.0% Ni-doped $CuGeO_3$, when the magnetic field is applied parallel to the b axis.

IV. DISCUSSION

Let us discuss why the spin-gap mode becomes Raman active in the impurity-doped $CuGeO_3$. When the dimerization parameter is one, $\gamma=1$, and the frustration parameter is zero, $\alpha=0$, in Eq. (1), the wave function of the ground state can be given as

$$|\varphi_\sigma\rangle = \cdots |\sigma\rangle_i |\sigma\rangle_{i+1} |\sigma\rangle_{i+2} \cdots, \tag{2}$$

where the spin-singlet dimer state $|\sigma\rangle_i$ of the $(2i-1,2i)$ dimer is $\frac{1}{\sqrt{2}}(|\uparrow\downarrow\rangle_{2i-1,2i} - |\downarrow\uparrow\rangle_{2i-1,2i})$. If the dimerization parameter is a little bit less than unity, the exchange-interaction term $(1-\gamma)J\boldsymbol{s}_{2i}\cdot\boldsymbol{s}_{2i+1}$ is treated as a perturbation Hamiltonian. Then the excited spin-singlet state

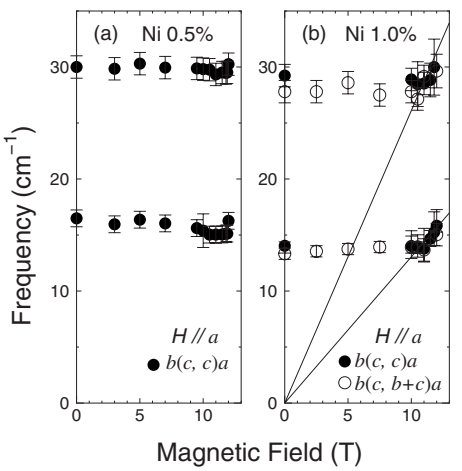

FIG. 9. Magnetic-field dependence of the frequency of the spin-gap mode and the peak position of the two-magnetic-excitation mode in (a) 0.5 and (b) 1.0% Ni-doped $CuGeO_3$, when the magnetic field is applied parallel to the a axis. The lines in (b) denote $1.4\mu_B H$ and $2.8\mu_B H$, where μ_B is the Bohr magneton, respectively.

$$|\varphi_{\sigma'}(i)\rangle = \cdots |\sigma\rangle_{i-1}|\sigma'\rangle_{i,i+1}|\sigma\rangle_{i+2}\cdots \tag{3}$$

is mixed to the unperturbed ground state in $\mathcal{O}[(1-\gamma)/(1+\gamma)]$ correction because

$$\boldsymbol{s}_{2i}\cdot\boldsymbol{s}_{2i+1}|\sigma\rangle_i|\sigma\rangle_{i+1} = \frac{\sqrt{3}}{4}|\sigma'\rangle_{i,i+1}. \tag{4}$$

Here the two-dimer state $|\sigma'\rangle_{i,i+1}$ represents the spin-singlet state other than $|\sigma\rangle_i|\sigma\rangle_{i+1}$ and is given as

$$|\sigma'\rangle_{i,i+1} = \frac{1}{\sqrt{3}}\{|\tau_{+1}\rangle_i|\tau_{-1}\rangle_{i+1} + |\tau_{-1}\rangle_i|\tau_{+1}\rangle_{i+1} - |\tau_0\rangle_i|\tau_0\rangle_{i+1}\}, \tag{5}$$

where $|\tau_{+1}\rangle_i = |\uparrow\uparrow\rangle_{2i-1,2i}$, $|\tau_0\rangle_i = \frac{1}{\sqrt{2}}(|\uparrow\downarrow\rangle_{2i-1,2i} + |\downarrow\uparrow\rangle_{2i-1,2i})$, and $|\tau_{-1}\rangle_i = |\downarrow\downarrow\rangle_{2i-1,2i}$, which are the $S_z=+1$ spin-triplet dimer state, the $S_z=0$ one, and the $S_z=-1$ one, of the $(2i-1,2i)$ dimer, respectively. Similarly,

$$\boldsymbol{s}_{2i-1}\cdot\boldsymbol{s}_{2i+1}|\sigma\rangle_i|\sigma\rangle_{i+1} = \boldsymbol{s}_{2i}\cdot\boldsymbol{s}_{2i+2}|\sigma\rangle_i|\sigma\rangle_{i+1} = -\frac{\sqrt{3}}{4}|\sigma'\rangle_{i,i+1}. \tag{6}$$

The wave function of the ground state is given as a linear combination of the spin-singlet states $|\varphi_\sigma\rangle$ and $|\varphi_{\sigma'}(i)\rangle$. Cowley *et al.*[36] discussed the magnetic excitation in the SP state of $CuGeO_3$ in this approximation. Moreover, Brenig[37] studied the SP state of $CuGeO_3$ using the bond-operator representation and discussed the magnetic excitations in detail, based on the limit of strong dimerization, taking the frustrated and interchain interactions into account.

Since the operator of $\boldsymbol{s}_i\cdot\boldsymbol{s}_j$ commutes with $(\boldsymbol{s}_i+\boldsymbol{s}_j)^2$ and $(s_i^z+s_j^z)$, not only the spin-singlet ground state but also all the excited state maintain the total spin S_{total} and its z component S_{total}^z even when γ approaches zero, and the frustration term is taken into consideration, as described by Eq. (1). There are also the spin-singlet states including two $|\sigma'\rangle$'s, three ones, and so on. Then the SP ground state $|\Psi_\sigma\rangle$ may be expanded by these spin-singlet states.

Within a framework of the dimer model, the $S_z=0$ triplet excited state $|\Psi_{\tau_0}(q_c)\rangle$ with a wave vector q_c along the chain direction is given as

$$|\Psi_{\tau_0}(q_c)\rangle = \frac{1}{\sqrt{N}}\sum_{i=1}^{N}(e^{-iq_c z_i}|\tau_0\rangle_i), \tag{7}$$

where all the dimer states correspond to those of the ground state $|\Psi_\sigma\rangle$ except for $|\tau_0\rangle$ at ith dimmer site and are omitted in the notation, N is the number of dimers in a spin chain, and $z_i=2ic$ because of the doubling of the unit cell along the c axis. Here, c is the lattice parameter of the c axis.

Fleury and Loudon[38] presented the theory of Raman scattering by one- and two-magnon excitations. The first-order (one-magnon) Raman scattering can be explained by the spin-orbit interaction mechanism involving an electric-dipole coupling, which proceeds through a spin-orbit coupling in the magnetic ions. This mechanism states for example that incident light linearly polarized along z gives rise to scattered light which is right-circularly polarized in the xy plane. This effective Raman Hamiltonian can be written by the total spin operators $S_{\text{total}}^+ = S_{\text{total}}^x + iS_{\text{total}}^y$ and $S_{\text{total}}^- = S_{\text{total}}^x - iS_{\text{total}}^y$ in the SP system $[(s_{2i-1}^+ + s_{2i}^+)$ and $(s_{2i-1}^- + s_{2i}^-)$ in the dimer model]. This mechanism, therefore, does not work in the SP state because the total spin is quenched completely in the ground state.

In the second-order magnetic Raman process of magnetic materials, the exchange integral works between the pair of magnetic ions. This mechanism plays an essential role in the spin-singlet ground state because the total spin S_{total} and its z component S_{total}^z are conserved in this Raman process. The Raman Hamiltonian in the exchange-interaction mechanism is fundamentally given as[38–41]

$$\mathcal{H}_R = \sum_{\langle ij\rangle} F_{i,j}(\boldsymbol{E}_{\text{in}}\cdot\hat{\boldsymbol{a}}_{i,j})(\boldsymbol{E}_{\text{sc}}\cdot\hat{\boldsymbol{a}}_{i,j})\boldsymbol{s}_i\cdot\boldsymbol{s}_j, \tag{8}$$

where $\boldsymbol{E}_{\text{in}}$ and $\boldsymbol{E}_{\text{sc}}$ are the unit vectors of the electric fields of the incident and scattered lights, respectively. Here $\hat{\boldsymbol{a}}_{i,j}$ is a unit vector connecting $\boldsymbol{s}_i$ and $\boldsymbol{s}_j$ and is parallel to the c axis in the one-dimensional spin-chain structure of $CuGeO_3$, and $F_{i,j}$ is the matrix element for the Raman process accompanied by simultaneous changes in the spin components of the interacting Cu^{2+} ions at ith and jth sites. Therefore we observe magnetic excitations in the (c,c) polarization, which are the totally symmetric A_g modes in the SP phase of $CuGeO_3$. For the alternating spin chain like the SP state of $CuGeO_3$, the Raman Hamiltonian in the (cc) polarization, which is derived from Eq. (8) and has a similar form to Eq. (1), is given as

$$\mathcal{H}_R^{\text{chain}} = F_0\sum_i\{(1+\gamma')\boldsymbol{s}_{2i-1}\cdot\boldsymbol{s}_{2i} + (1-\gamma')\boldsymbol{s}_{2i}\cdot\boldsymbol{s}_{2i+1} + \alpha'(\boldsymbol{s}_{2i-1}\cdot\boldsymbol{s}_{2i+1} + \boldsymbol{s}_{2i}\cdot\boldsymbol{s}_{2i+2})\}, \tag{9}$$

where γ' and α' are expected to be about as large as γ and α, respectively, and F_0 originates from $F_{i,j}$ in Eq. (8). If $\gamma=\gamma'$ and $\alpha=\alpha'$, the Raman Hamiltonian commutes with Eq. (1) and there would be no Raman scattering.[40,41] The parameters γ and α were estimated as 0.014 and 0.24–0.36, respectively.[42–44] The following terms

$$\mathcal{H}_R^{\text{chain}} \simeq F_0(\alpha'-\alpha)\sum_i(\boldsymbol{s}_{2i-1}\cdot\boldsymbol{s}_{2i+1} + \boldsymbol{s}_{2i}\cdot\boldsymbol{s}_{2i+2}), \tag{10}$$

works substantially in the Raman process of pure $CuGeO_3$. The SP ground state $|\Psi_\sigma\rangle$ includes pairs of dimers $|\sigma\rangle_i|\sigma\rangle_{i+1}$, as mentioned before. Using Eq. (6), the spin-singlet excited dimmer state $|\sigma'\rangle$, i.e., the spin-singlet excited state $|\Psi_{\sigma'}(q_c=0)\rangle$, can be created by Raman scattering and it may be approximately written by two triplet magnetic excitations near $2\Delta(T)$,

$$\begin{aligned}|\Psi_{\sigma'}(q_c=0)\rangle &= \frac{1}{\sqrt{N}}\sum_{i=1}^{N}|\sigma'\rangle_{i,i+1}\\ &\sim \frac{1}{\sqrt{3N}}\sum_{q_c'}\left\{\left|\Psi_{\tau_{+1}}\left(-\frac{\pi}{c}+q_c'\right)\right\rangle\left|\Psi_{\tau_{-1}}\left(\frac{\pi}{c}-q_c'\right)\right\rangle\right.\\ &\quad + \left|\Psi_{\tau_{-1}}\left(-\frac{\pi}{c}+q_c'\right)\right\rangle\left|\Psi_{\tau_{+1}}\left(\frac{\pi}{c}-q_c'\right)\right\rangle\\ &\quad \left. - \left|\Psi_{\tau_0}\left(-\frac{\pi}{c}+q_c'\right)\right\rangle\left|\Psi_{\tau_0}\left(\frac{\pi}{c}-q_c'\right)\right\rangle\right\},\end{aligned} \tag{11}$$

when interactions between magnetic excitations are weak. Its spectrum shows approximately the density of states of the overtone magnetic excitations near $2\Delta(T)$, which is described by $\sqrt{\omega-2\Delta(T)}$, where ω is the frequency (energy).[25] It reflects the three dimensionality in magnetic property because the interchain interactions are not weak in $CuGeO_3$.[46] When attractive interactions are strong between the spin-triplet excited states, i.e., when γ is small and/or α is large, the two-magnetic-excitation bound state is created just below double the SP-gap energy and the Raman spectrum shows an asymmetric peak with a tail in the high-frequency region.[27] Moreover, it neither splits nor shifts under magnetic fields in the SP phase because this state is spin-singlet.

Next let us consider the case when $CuGeO_3$ is doped with Ni^{2+} ions. The Ni^{2+} ions locally destroy the nonmagnetic spin-singlet state and consequently the local magnetic field involving the staggered magnetic field and the uniform average one emerges but attenuates far from the Ni^{2+} ions. This magnetic field originates from the AF magnetic moments near the impurities. The local AF order extends to approximately ten correlated spins of a chain.[17] When the effective local magnetic fields B_{2i-1} and B_{2i} $(=h_{2i}/g\mu_B)$ are applied along the z direction at the spins of the $(2i-1,2i)$ dimer near the Ni^{2+} ion, the simplified Hamiltonian in a dimer can be written as

$$\mathcal{H}_i = \frac{3}{4}\Delta_0 + \Delta_0 \boldsymbol{s}_{2i-1}\cdot\boldsymbol{s}_{2i} + \mathcal{H}_i', \tag{12}$$

where g and μ_B are the g factor and the Bohr magneton, respectively, the energies of the unperturbed spin-singlet ground state $|\sigma\rangle$ and spin-triplet excited state $|\tau\rangle$ in the dimer are given as 0 and Δ_0, respectively, and

$$\mathcal{H}_i' = h_{2i-1}s_{2i-1}^z + h_{2i}s_{2i}^z = h_i^{\mathrm{av}}(s_{2i-1}^z + s_{2i}^z) + h_i^{\mathrm{st}}(s_{2i-1}^z - s_{2i}^z). \tag{13}$$

Here

$$h_i^{\mathrm{av}} = \frac{h_{2i-1}+h_{2i}}{2}, \quad h_i^{\mathrm{st}} = \frac{h_{2i-1}-h_{2i}}{2}. \tag{14}$$

Since the average magnetic field h_i^{av} does not play an important role and is much weaker than h_i^{st}, we neglect it hereafter. The staggered magnetic field h_i^{st} mixes the spin-singlet dimer state $|\sigma\rangle_i$ and the $S_z=0$ triplet dimer state $|\tau_0\rangle_i$, and then we consider the following state:

$$|\phi_{\mathrm{g(e)}}\rangle_i = \frac{1}{\sqrt{1+d_i^{\mathrm{g(e)}2}}}\{|\sigma\rangle_i + d_i^{\mathrm{g(e)}}|\tau_0\rangle_i\}. \tag{15}$$

We obtain the energies E_i^{g} of the ground state $|\phi_{\mathrm{g}}\rangle_i$ and E_i^{e} of the excited state $|\phi_{\mathrm{e}}\rangle_i$,

$$E_i^{\mathrm{g}} = \frac{\Delta_0 - \sqrt{\Delta_0^2 + 4h_i^{\mathrm{st}2}}}{2},$$

$$E_i^{\mathrm{e}} = \frac{\Delta_0 + \sqrt{\Delta_0^2 + 4h_i^{\mathrm{st}2}}}{2}, \tag{16}$$

and

$$d_i^{\mathrm{g}} = \frac{E_i^{\mathrm{g}}}{h_i^{\mathrm{st}}}, \quad d_i^{\mathrm{e}} = \frac{E_i^{\mathrm{e}}}{h_i^{\mathrm{st}}}. \tag{17}$$

The above result in a dimer, therefore, suggests that the SP ground state $|\Psi_\sigma\rangle$ and the $S_z=0$ triplet excited state $|\Psi_{\tau_0}(q_c)\rangle$ with $q_c=\pi/c$ are mixed with each other by impurities of Ni^{2+} ions. This is the origin of activation of the spin-gap mode. It should be noted that the $S_z=\pm1$ triplet dimer states $|\tau_{\pm1}\rangle$ are not mixed with the singlet dimer state, leading to that $|\Psi_{\tau_{\pm1}}(q_c=\pi/c)\rangle$ states remain Raman inactive. In case of the magnon Bose-Einstein condensed phase of the spin-dimer system $TlCuCl_3$ under high magnetic fields, on the other hand, the mixing of the $S_z=\pm1$ spin-triplet states into the spin-singlet ground state activates the one-magnon Raman scattering.[45]

When the staggered magnetic field exists, the gap energy, $E_i^{\mathrm{e}}-E_i^{\mathrm{g}}$, is larger than Δ_0. Using $h_i^{\mathrm{st}}\simeq 2J(1-\alpha)s_i^z$, we roughly estimate the average of the staggered magnetic field $\langle h_i^{\mathrm{st}}\rangle \sim 0.22\Delta_0$. Here we used $\Delta_0=2.0$ meV,[46] $J=10.4$ meV,[46] $\alpha \sim 0.3$,[42–44] $g\sim 2.0$, which was obtained for the b axis in 0.5% Ni-doped $CuGeO_3$,[23] and the result of the effective staggered magnetic moment, $g\mu_B\langle s_i^z\rangle \sim 0.06\mu_B$, in 1.7% Ni-doped $CuGeO_3$.[35] Taking into account the facts that the lattice distortion δ is reduced in the impurity-doped $CuGeO_3$ and δ is proportional to $\Delta(0)^{3/2}$,[31,47] the average gap energy, $\langle E_i^{\mathrm{e}}-E_i^{\mathrm{e}}\rangle$, probably becomes smaller than Δ_0. The energy of the spin-gap mode $\Delta(0)$, which was obtained in the present experiment, corresponds to $\langle E_i^{\mathrm{e}}-E_i^{\mathrm{g}}\rangle$ and is a few cm^{-1} smaller than Δ_0 of pure $CuGeO_3$.

The transition from the ground state to the excited state becomes allowed in the exchange-interaction Raman process, which may be created by the Raman Hamiltonian of Eq. (9) in Ni-doped $CuGeO_3$, instead of Eq. (10) in the two-magnetic-excitation mode, and the matrix element in a dimer is given as

$$\langle\phi_{\mathrm{e}}|\mathcal{H}_R^{\mathrm{chain}}|\phi_{\mathrm{g}}\rangle_{i,i} = -F_0(1+\gamma')\frac{h_i^{\mathrm{st}}}{\sqrt{\Delta_0^2+4h_i^{\mathrm{st}2}}}. \tag{18}$$

Using $\gamma'\sim\gamma\sim 1.4\times10^{-2}$ and $|\alpha-\alpha'|\sim\alpha\sim0.3$,[42–44] we roughly estimate

$$(1+\gamma')\frac{\langle h_i^{\mathrm{st}}\rangle}{\sqrt{\Delta_0^2+4\langle h_i^{\mathrm{st}}\rangle^2}} \sim 0.2, \tag{19}$$

which is nearly equal to $|\alpha-\alpha'|$. The local AF order extends to approximately ten correlated spins of a chain in the vicinity of Ni^{2+} ion.[17] Probably, the local AF order is also induced in the adjacent chains because the momentum conservation nearly holds in the Raman process from the spin-gap mode, as will be discussed later. Then the Raman intensity of the spin-gap mode is nearly equal to that of the two-magnetic-excitation mode, and consequently it was observed in the (c,c) polarization configuration, even though the impurity concentration is very small, i.e., a few percent.

With increasing the concentration of Ni^{2+} ions the locally correlated antiferromagnetic (AF) spins are increased, resulting in a decrease in the two-magnetic-excitation mode in Raman intensity together with an increase in the spin-gap

mode. It, however, hardly increased when the Ni concentration was changed from 0.5% to 1.0% because the growth of the long-range spin-Peierls (SP) order was arrested.

The correlated spin order around a Ni^{2+} ion probably extends to more than a few tens spins not only within a chain but also in the adjacent chains. The $S_z=0$ spin-triplet excited states $|\Psi_{\tau_0}(q_c)\rangle$ near $q_c=\pi/c$ are mixed with the SP ground state $|\Psi_\sigma\rangle$. Moreover, the momentum conservation along the a and b axes is approximately maintained in the Raman process from the spin-gap mode. Among the one-dimensional spin chains, a ferromagnetic and an AF interchain interaction work along the a (x) and b (y) axes, respectively.[46] Then the SP state has a lattice modulation with $(q_a,q_b)=(0,1)$, since the spin chains are located at $(x,y)=(\ell a,nb/2)$, where ℓ and n are integers. The spin excitation, which has a phase factor of $\exp(i\frac{2\pi}{b}y)$ along the b axis, is created by the exchange-interaction Raman process. Thus we observed the SP-gap excitation at (0,1,0.5) point, i.e., at the magnetic zone center, which has the minimum energy in the reciprocal lattice space, taking the doubling of the unit cell along the c (z) direction into account.[46] Meanwhile, the SP-gap excitation at (0,0,0.5) point at 44 cm^{-1} is infrared-red active even in pure $CuGeO_3$ when the polarization of the far-infrared light $\boldsymbol{E}$ is along the b axis.[48]

It is worthwhile to consider the emergence of the spin-gap mode by impurity doping in terms of Dzyaloshinskii-Moriya (DM) exchange interaction:

$$\mathcal{H}_{\mathrm{DM}}=\sum_i \boldsymbol{D}\cdot(\boldsymbol{s}_i\times\boldsymbol{s}_{i+1}). \tag{20}$$

The DM interaction may appear near the impurities because the inversion symmetry is broken there. When the DM vector $\boldsymbol{D}$ is parallel to the applied magnetic field, the $S_z=0$ spin-triplet dimer state $|\tau_0\rangle$ is mixed with the spin-singlet ground state $|\sigma\rangle$. On the other hand, when $\boldsymbol{D}$ is perpendicular to the applied magnetic field, the $S_z=\pm 1$ spin-triplet dimer states $|\tau_\pm\rangle$ are mixed with the spin-singlet ground state $|\sigma\rangle$.[49] By means of Raman scattering, Gozar and Blumberg[50] observed a splitting of the spin-gap mode between the singlet ground state and the excited triplet one in NaV_2O_5 when the applied magnetic field was perpendicular to the DM vector, and no splitting when the applied magnetic field was parallel to the DM vector. At least, either of the magnetic fields along the a axis or the b one is not parallel to the DM vector in the present experiment, and then we should observe a splitting of the spin-gap mode. Therefore the present results cannot be explained by the DM interaction. When the DM interaction exists, the Raman Hamiltonian with the same form of Eq. (20) should be taken into consideration. But the present results cannot be understood in terms of this Raman Hamiltonian.

When a magnetic field is applied parallel to the local staggered field, i.e., the locally correlated AF moments, the spin-gap mode neither splits nor shifts. However, the frequency shift and the splitting should be observed when an applied magnetic field is perpendicular to the local staggered field because the $S_z=\pm 1$ spin-triplet states are mixed into the singlet state. The spins of Ni^{2+} ions is directed nearly along the a axis because of the single-ion magnetic anisotropy in the AF ordered state.[18,19,21–23] Then it is expected that the locally correlated AF moments in the vicinity of the Ni^{2+} ions, i.e., the staggered magnetic field in the vicinity of the Ni^{2+} ions is also nearly parallel to the a axis in the SP state. However, the easy-axis anisotropy was estimated to be very weak.[21,23] On the other hand, the easy axis is along the c axis in the AF ordered state of nonmagnetic-impurity-doped $CuGeO_3$.[2] Probably, the local AF moments, which are located far from a Ni^{2+} ion, tend to be parallel to the c axis in Ni-doped $CuGeO_3$. Then the staggered magnetic field may be easily turned toward the direction of the external magnetic field at a low magnetic field, in particular when the AF long-range order is not formed. Therefore, the spin-gap mode neither split nor shifted in the SP phase when magnetic fields were applied parallel to the a and b axes. Contrary to Raman scattering, the splitting of the SP gap under magnetic fields was observed by neutron scattering.[51]

Under high magnetic fields, the incommensurate (IC) state with a finite magnetization[24] is formed since its energy is lower than the SP state. Just above H_c the IC state can be described as discommensuration possessing domain walls and the intervening commensurate lattices, thus forming the soliton lattice.[52–56] The magnetic soliton possessing $s=1/2$ in the IC phase involves the staggered and average magnetic moments.[55] Then the above discussion is also applicable to the IC phase. The spin-gap mode, therefore, becomes observable even in the IC phase of pure $CuGeO_3$ by Raman scattering.[29,30,33] With increasing magnetic field, the distance between the solitons is reduced.[56] Then the Raman intensity of the two-magnetic-excitation mode decreases, while that of the spin-gap mode increases. Moreover, their frequencies increase.

The spin-gap mode was also observed in nonmagnetic-impurity-doped $CuGeO_3$, i.e., Zn-, Mg-, and Si-doped $CuGeO_3$, by Raman scattering.[27,28,31] These impurities also induced the emergence of local staggered magnetization, resulting in the mixing between the spin-singlet ground state and the $S_z=0$ spin-triplet excited state. Then the spin-gap mode becomes allowed in the exchange-interaction Raman process.

Els *et al.*[28,32] interpreted the spin-gap mode in terms of a dopant-bound spinon. It moves far from the impurity through the exchange-interaction Raman process of Eq. (9). In Ni-doped sample the spinon bound to Ni^{2+} ion with an $s=1$ spin hardly moves because it is expected to cost higher energy when compared with the case of nonmagnetic impurity, which denies this interpretation. Loa *et al.*[29,30] considered the following process, assuming a spinon at $(2i+1)$th site in the vicinity of the dopant impurity:

$$\boldsymbol{s}_{2i}\cdot\boldsymbol{s}_{2i+1}|\sigma\rangle_i|\uparrow\rangle_{2i+1}=\frac{1}{2\sqrt{2}}|\tau_{+1}\rangle_i|\downarrow\rangle_{2i+1}-\frac{1}{4}|\tau_0\rangle_i|\uparrow\rangle_{2i+1}. \tag{21}$$

Taking into consideration the fact that the locally correlated AF spins are created near the impurities, the term of $|\tau_{+1}\rangle_i|\downarrow\rangle_{2i+1}$ in Eq. (21) representing the reverse of the spin at $(2i+1)$th site should possess a higher energy because the spin becomes parallel to the nearest neighbor one at $(2i$

+2)th site. Since it has not been observed yet by Raman scattering, this interpretation is not applicable to the present case in $CuGeO_3$.

V. CONCLUSION

We studied Raman scattering in Ni-doped $CuGeO_3$ crystals under high magnetic fields at low temperatures. The 0.5 and 1.0% doped samples undertook the spin-Peierls transition (SP) but the 2.0 and 2.8% doped samples do not. However, the folded-phonon mode was weakly observed even in the samples, which do not have the SP transition, indicating the existence of the short-range lattice dimerization. The two-magnetic-excitation mode was observed in the SP phase. Then it was not observed in 2.0 and 2.8% doped samples. The spin-gap mode appeared only in the SP state of Ni-doped sample. With increasing Ni concentration, the frequency of the spin-gap mode decreased. The incommensurate (IC) phase, where the frequencies of the spin-gap mode and the two-magnetic-excitation mode increase with increasing magnetic field, was observed above $H_c \simeq 11.5$ T in 1.0% Ni-doped sample. The critical magnetic field H_c decreases with increasing Ni concentration.

The impurity dopings induce a staggered magnetic field. The activation of the spin-gap mode is interpreted in terms of a mixing between the singlet ground state and the $S_z=0$ triplet excited one by the staggered magnetic field.

This interpretation is applicable to the spin-gap mode not only in the nonmagnetic-impurity-doped samples, i.e., Zn-, Mg-, and Si-doped $CuGeO_3$, but also in the magnetic soliton lattice of the incommensurate state under high magnetic fields.

Taking into account the case of the magnon Bose-Einstein condensed phase in $TlCuCl_3$, we conclude that Raman scattering from one magnetic excitation is generally activated by a mixing between the spin-singlet ground and spin-triplet excited states in the spin-gap systems.

ACKNOWLEDGMENTS

We thank K. Uchinokura for fruitful discussion.

*t-sekine@sophia.ac.jp

[1] M. Hase, I. Terasaki, and K. Uchinokura, Phys. Rev. Lett. **70**, 3651 (1993).
[2] For review, K. Uchinokura, J. Phys.: Condens. Matter **14**, R195 (2002).
[3] M. Hase, I. Terasaki, Y. Sasago, K. Uchinokura, and H. Obara, Phys. Rev. Lett. **71**, 4059 (1993).
[4] S. B. Oseroff, S.-W. Cheong, B. Aktas, M. F. Hundley, Z. Fisk, and L. W. Rupp, Jr., Phys. Rev. Lett. **74**, 1450 (1995).
[5] M. Hase, N. Koide, K. Manabe, Y. Sasago, K. Uchinokura, and A. Sawa, Physica B (Amsterdam) **215**, 164 (1995).
[6] J.-G. Lussier, S. M. Coad, D. F. McMorrow, and D. McK. Paul, J. Phys.: Condens. Matter **7**, L325 (1995).
[7] J. P. Renard, K. Le. Dang, P. Veillet, G. Dhalenne, A. Revcolevschi, and L. P. Regnault, Europhys. Lett. **30**, 475 (1995).
[8] M. Poirier, R. Beaudry, M. Castonguay, M. L. Plumer, G. Quirion, F. S. Razavi, A. Revcolevschi, and G. Dhalenne, Phys. Rev. B **52**, R6971 (1995).
[9] L. P. Regnault, J.-P. Renard, G. Dhalenne, and A. Revcolevschi, Europhys. Lett. **32**, 579 (1995).
[10] M. Hase, K. Uchinokura, R. J. Birgeneau, K. Hirota, and G. Shirane, J. Phys. Soc. Jpn. **65**, 1392 (1996).
[11] Y. Sasago, N. Koide, K. Uchinokura, M. C. Martin, M. Hase, K. Hirota, and G. Shirane, Phys. Rev. B **54**, R6835 (1996).
[12] M. C. Martin, M. Hase, K. Hirota, G. Shirane, Y. Sasago, N. Koide, and K. Uchinokura, Phys. Rev. B **56**, 3173 (1997).
[13] V. N. Glazkov, A. I. Smirnov, K. Uchinokura, and T. Masuda, Phys. Rev. B **65**, 144427 (2002).
[14] V. N. Glazkov, A. I. Smirnov, H. A. Krug von Nidda, A. Loidl, K. Uchinokura, and T. Masuda, Phys. Rev. Lett. **94**, 057205 (2005).
[15] T. Masuda, A. Fujioka, Y. Uchiyama, I. Tsukada, and K. Uchinokura, Phys. Rev. Lett. **80**, 4566 (1998).
[16] H. Fukuyama, T. Tanimoto, and M. Saito, J. Phys. Soc. Jpn. **65**, 1182 (1996).
[17] K. M. Kojima, Y. Fudamoto, M. Larkin, G. M. Luke, J. Merrin, B. Nachumi, Y. J. Uemura, M. Hase, Y. Sasago, K. Uchinokura, Y. Ajiro, A. Revcolevschi, and J. P. Renard, Phys. Rev. Lett. **79**, 503 (1997).
[18] N. Koide, Y. Sasago, T. Masuda, and K. Uchinokura, Czech. J. Phys. **46**, 1981 (1996).
[19] T. Masuda, N. Koide, and K. Uchinokura, Prog. Theor. Phys. Suppl. **145**, 306 (2002).
[20] M. Weiden, W. Richter, R. Hauptmann, C. Geibel, and F. Steglich, Physica B (Amsterdam) **233**, 153 (1997).
[21] P. E. Anderson, J. Z. Liu, and R. N. Shelton, Phys. Rev. B **57**, 11492 (1998).
[22] B. Grenier, P. Monod, M. Hagiwara, M. Matsuda, K. Katsumata, S. Clément, J. P. Renard, A. L. Barra, G. Dhalenne, and A. Revcolevschi, Phys. Rev. B **65**, 094425 (2002).
[23] V. N. Glazkov, A. I. Smirnov, O. A. Petrenko, D. McK. Paul, A. G. Vetkin, and R. M. Eremina, J. Phys.: Condens. Matter **10**, 7879 (1998).
[24] M. Hase, I. Terasaki, K. Uchinokura, M. Tokunaga, N. Miura, and H. Obara, Phys. Rev. B **48**, 9616 (1993).
[25] H. Kuroe, T. Sekine, M. Hase, Y. Sasago, K. Uchinokura, H. Kojima, I. Tanaka, and Y. Shibuya, Phys. Rev. B **50**, 16468 (1994).
[26] H. Kuroe, J. Sasaki, T. Sekine, T. Masuda, N. Koide, I. Tsukada, and K. Uchinokura, J. Phys. Soc. Jpn. **68**, 2046 (1999).
[27] T. Sekine, H. Kuroe, J. Sasaki, Y. Sasago, N. Koide, K. Uchinokura, and M. Hase, J. Phys. Soc. Jpn. **67**, 1440 (1998).
[28] G. Els, G. S. Uhrig, P. Lemmens, H. Vonbreg, P. H. M. van Loosdrecht, G. Güntherodt, O. Fujita, J. Akimitsu, G. Dhalenne, and A. Revcolevschi, Europhys. Lett. **43**, 463 (1998).
[29] I. Loa, S. Gronemer, C. Thomsen, and R. K. Kremer, Solid State Commun. **111**, 181 (1999).
[30] I. Loa, Doctor Thesis, Technische Universität Berlin, 1999.

[31] Y. Tanokura, Y. Oono, S. Ikeda, H. Kuroe, T. Sekine, T. Masuda, and K. Uchinokura, Phys. Rev. B **68**, 054412 (2003).
[32] P. Lemmens, G. Gütherodt, and C. Gros, Phys. Rep. **375**, 1 (2003).
[33] I. Loa, S. Gronemer, C. Thomsen, and R. K. Kremer, Z. Phys. Chem. **333-342**, 607 (1997).
[34] H. Völlenkle, A. Wittmann, and H. Nowotny, Monatsch. Chem. **98**, 1352 (1967).
[35] S. Coad, O. Petrenko, D. McK. Paul, B. Fåk, J.-G. Lissier, and D. F. McMorrow, Physica B (Amsterdam) **239**, 350 (1997).
[36] R. A. Cowley, B. Lake, and D. A. Tennant, J. Phys.: Condens. Matter **8**, L179 (1996).
[37] W. Brenig, Phys. Rev. B **56**, 14441 (1997).
[38] P. A. Fleury and R. Loudon, Phys. Rev. **166**, 514 (1968).
[39] J. B. Parkinson, J. Phys. C **2**, 2012 (1969).
[40] V. N. Muthukumar, C. Gros, W. Wenzel, R. Valentí, P. Lemmens, B. Eisener, G. Güntherodt, M. Weiden, C. Geibel, and F. Steglich, Phys. Rev. B **54**, R9635 (1996).
[41] C. Gros, W. Wenzel, A. Fledderjohann, P. Lemmens, M. Fischer, G. Güntherodt, M. Weiden, C. Geibel, and F. Steglich, Phys. Rev. B **55**, 15048 (1997).
[42] J. Riera and A. Dobry, Phys. Rev. B **51**, 16098 (1995).
[43] G. Castilla, S. Chakravarty, and V. J. Emery, Phys. Rev. Lett. **75**, 1823 (1995).
[44] H. Kuroe, J. I. Sasaki, T. Sekine, N. Koide, Y. Sasago, K. Uchinokura, and M. Hase, Phys. Rev. B **55**, 409 (1997).
[45] H. Kuroe, K. Kusakabe, A. Oosawa, T. Sekine, F. Yamada, H. Tanaka, and M. Matsumoto, Phys. Rev. B **77**, 134420 (2008).
[46] M. Nishi, O. Fujita, and J. Akimitsu, Phys. Rev. B **50**, 6508 (1994).
[47] M. C. Cross and D. S. Fisher, Phys. Rev. B **19**, 402 (1979).
[48] K. Takehana, T. Takamasu, M. Hase, G. Kido, and K. Uchinokura, Phys. Rev. B **62**, 5191 (2000).
[49] T. Rõõm, D. Hüvonen, U. Nagel, Y.-J. Wang, and R. K. Kremer, Phys. Rev. B **69**, 144410 (2004).
[50] A. Gozar and G. Blumberg, in *Frontiers in Magnetic Materials*, edited by A. V. Narlikar (Springer-Verlag, Berlin, 2005), p. 697.
[51] O. Fujita, J. Akimitsu, M. Nishi, and K. Kakurai, Phys. Rev. Lett. **74**, 1677 (1995).
[52] V. Kiryukhin and B. Keimer, Phys. Rev. B **52**, R704 (1995).
[53] V. Kiryukhin, B. Keimer, J. P. Hill, and A. Vigliante, Phys. Rev. Lett. **76**, 4608 (1996).
[54] V. Kiryukhin, B. Keimer, J. P. Hill, S. M. Coad, and D. McK. Paul, Phys. Rev. B **54**, 7269 (1996).
[55] M. Horvatić, Y. Fagot-Revurat, C. Berthier, G. Dhalenne, and A. Revcolevschi, Phys. Rev. Lett. **83**, 420 (1999).
[56] H. M. Rønnow, M. Enderle, D. F. McMorrow, L. P. Regnault, G. Dhalenne, A. Revcolevschi, A. Hoser, K. Prokes, P. Vorderwisch, and H. Schneider, Phys. Rev. Lett. **84**, 4469 (2000).